Communication

High-resolution local field spectroscopy with internuclear correlations

Alexander A. Nevzorov

Department of Chemistry, North Carolina State University, 2620 Yarbrough Drive, Raleigh, NC 27695-8204, USA

ABSTRACT

Establishing correlations among distant (>3 Å) spins remains an outstanding problem for both spectral assignment and elucidation of interhelical contacts in solid-state NMR of oriented membrane proteins. Here we present a pulse sequence which incorporates the previously established mismatched Hartmann–Hahn mixing of dilute spins via the proton bath together with high-resolution local field spectroscopy. In addition to providing structural information, the use of dipolar couplings in the indirect dimension helps eliminate the spectral crowdedness compared to the standard homonuclear correlation techniques. The proposed pulse sequence may find its use in assigning protein spectra in uniaxially oriented membrane environments.

© 2009 Elsevier Inc. All rights reserved.

Solid-state NMR of uniaxially oriented samples represents a powerful method for determining the structures of membrane proteins in their native lipid environment. Using the method of NMR orientational restraints, structures of several membrane proteins have been determined to date by solid-state NMR of macroscopically aligned samples. These include, but are not limited to: gramicidin [1], the M2 domain of the influenza A virus [2], AchR M2 domain [3], fd [4,5], pf1 [6,7] phage coat proteins, VPU (from HIV-1) [8], phospholamban [9], and MerF [10]. However, usually the assignment of these spectra is carried out by a laborious preparation of selectively labeled samples followed by discerning the resonance patterns using the so-called "shotgun approach" [11]. In order to be able to extend these methods to non-helical domains it is necessary to establish a pure spectroscopic method of assignment. While the dilute-spin exchange methods based on proton-driven spin diffusion [12] have been used in the past for this purpose [13], they are relatively slow and do not establish correlations among more distant (>5 Å) spins. Alternatively, cross-relaxation driven spin diffusion (CRDSD) method [14] could be employed to speed up the magnetization transfer between the directly coupled low spins. Recently, a novel method [15] based on magnetization transfer under the mismatched Hartmann–Hahn (MMHH) conditions has been proposed, which allows one to establish correlations within several milliseconds among the weak (e.g. ^{15}N) spins separated by as much as 6.7 Å in NMR of static solids. Here, the magnetization transfer is mediated by the spatially uniform proton bath by analogy with the method established in MAS [16], and does not depend on the direct interaction between the weak spins, unlike the dilute-spin exchange [13] or

the CRDSD method [14]. The latter property is especially beneficial for ^{15}N NMR of membrane proteins, where the ^{15}N–^{15}N dipolar coupling constants between the neighboring amide sites are typically less than 50 Hz (which corresponds to a distance of about 3 Å), and the additional angular dependence further decreases the dipolar couplings. The MMHH method of transferring magnetization opens up new venues for a different class of experiments in solid-state NMR of static samples, one example of which is presented below. One of the motivations is to reduce the spectral crowding caused by the peaks on the main diagonal by replacing the chemical shift evolution by the heteronuclear dipolar evolution in the indirect dimension similarly to the ideas introduced in solution-NMR NOESY- and TOCSY-HSQC experiments [17]. In the present work, the spin correlations are established by inserting a mixing period between the two dimensions, which extends the classical separated local field experiments [18,19] to a next level potentially yielding both sufficient structural information and assignment in a single NMR experiment.

The pulse sequence implementing these objectives is shown in Fig. 1. First, the cross-polarization (CP) is used to enhance magnetization of the dilute (^{15}N) nuclei. Then the SAMPI4 pulse sequence [20] is applied to evolve the heteronuclear (^1H–^{15}N) dipolar couplings. The Z-filter is subsequently applied to: (a) destroy any residual proton magnetization; (b) allow for the probe to cool down before a long (several ms) mixing period is applied followed by proton decoupling. After the stored ^{15}N magnetization is brought back to the x-axis, the mismatched Hartmann–Hahn scheme is used to establish spectral correlations among the weak spins [15]. In the present work, however, we applied the proton rf field above the match value (a justification for this is given
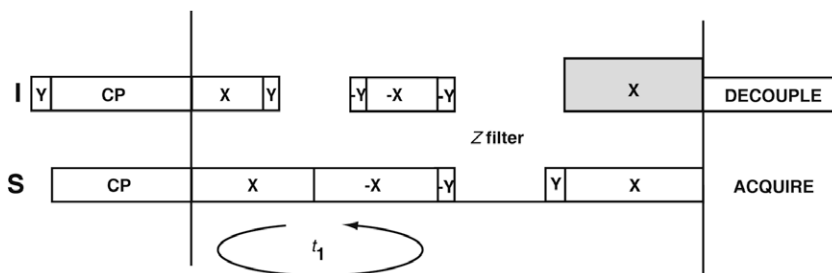
E-mail address: alex_nevzorov@ncsu.edu

Fig. 1. Two-dimensional pulse sequence for the high-resolution separated local filed spectroscopy that simultaneously establishes internuclear correlations. Cross-polarization is used to enhance the magnetization on the ^{15}N side. The SAMPI4 pulse sequence, which is 180°-cycled between odd and even dwells, is applied to evolve the heteronuclear dipolar couplings. After the Z-filter, the stored ^{15}N magnetization is brought back along the x-axis. The mismatched Hartmann–Hahn scheme with the proton rf field above the CP match value is applied. Finally, the ^{15}N chemical shift is detected under the conditions of proton decoupling.

below). Finally, the direct dimension is detected under the conditions of proton decoupling [21]. Two overlaid spectra acquired for an n-acetyl Leucine (NAL) single crystal are shown in Fig. 2. The spectrum with the black contour lines is the conventional SAMPI4 spectrum, which allows one to distinguish the main peaks from the cross peaks. The SAMPI4 spectrum is overlaid with the "exchanged" SAMPI4 spectrum (gray contour lines) acquired using the pulse sequence of Fig. 1. As can be seen, all the twelve cross peaks are established among the four main peaks. It should be noted that these cross peaks are purely intermolecular since there is only one ^{15}N site per NAL molecule. Furthermore, the magnetization transfer occurs over the distances 6.5–6.7 Å as determined from the NAL X-ray structure ACLLEU01 [22], which renders the direct coupling constant between the closest ^{15}N sites as little as 4.5 Hz or less. No cross peaks could be observed under these conditions using the dilute-spin exchange method even after up to 15 s mixing time [15]. Another observation is that the buildup of cross peaks occurs more effectively when the proton rf amplitude is set above the Hartmann–Hahn match value. Let us consider a many-body system consisting of two low spins $S^{(1)}$ and $S^{(2)}$ and N protons $I^{(n)}$ which evolves under the Hamiltonian:

$$H = \omega_S \left(S_x^{(1)} + S_x^{(2)} \right) + \omega_I I_x^{\text{total}} + \sum_{n=1}^{N} \left(a_{1n} S_z^{(1)} I_z^{(n)} + a_{2n} S_z^{(2)} I_z^{(n)} \right) + H_{\text{like}}$$

(1)

where the interactions among the protons are given by:

$$H_{\text{like}} = \sum_{i<j} b_{ij} \left[I_z^{(i)} I_z^{(j)} - \frac{1}{4} \left(I_+^{(i)} I_-^{(j)} + I_-^{(i)} I_+^{(j)} \right) \right]$$

(2)

The interaction coefficients a_{ij} and b_{ij} corresponding to the dipolar couplings between the nitrogens and the protons, and among the protons themselves, respectively, have been calculated from the atomic coordinates of the NAL crystal structure [22] at arbitrary orientation (ACLLEU01, deposition 624793). The CP amplitude B_1 (in frequency units) was set to $\omega_S = 60$ kHz. The transferred intensity between the spins $S^{(1)}$ and $S^{(2)}$ was calculated numerically using the quasistationary solution for the density matrix equation (e.g. by setting $t = 100$ ms):

$$G(t) = \text{Trace} \left(S_x^{(2)} e^{-iHt} S_x^{(1)} e^{iHt} \right)$$

(3)

Note that in the simplest case of two weak spins interacting with a single proton, the following truncated Hamiltonian is obtained in the doubly tilted frame (cf. Ref. [15]):

$$H_T = -\Delta\omega I_z + \frac{a_1}{4} \left[S_+^{(1)} I_- + S_-^{(1)} I_+ \right] + \frac{a_2}{4} \left[S_+^{(2)} I_- + S_-^{(2)} I_+ \right]$$

(4)

where $\Delta\omega = \omega_S - \omega_I$ is the Hartmann–Hahn mismatch (in frequency units). Direct calculation gives the time evolution of the transferred magnetization as:

$$G(t) = \text{Trace} \left(S_z^{(2)} e^{-iH_Tt} S_z^{(1)} e^{iH_Tt} \right)$$
$$= \frac{a_1^2 a_2^2}{2\Omega(a_1^2 + a_2^2)} \left[\frac{\sin^2(\Omega+2\Delta\omega)t/8}{(\Omega+2\Delta\omega)/8} + \frac{\sin^2(\Omega-2\Delta\omega)t/8}{(\Omega-2\Delta\omega)/8} - \frac{\sin^2 \Omega t/4}{\Omega/4} \right]$$

(5)

where $\Omega = (a_1^2 + a_2^2 + 4\Delta\omega^2)^{1/2}$. Even for the simple three-spin system the analytical behavior of the transferred magnetization is rather complicated. In the absence of proton–proton interactions, the maximum intensity of the magnetization transfer is independent of $\Delta\omega$, and in the above three-spin case corresponds to $8a_1^2 a_2^2/(a_1^2 + a_2^2)^2$. In addition, for the three-spin system the behavior is oscillatory; whereas in a many-proton system quasistationary magnetization transfer is achieved [15]. Fig. 3 shows the result of the numerical calculation for the transferred magnetization in a 12-spin system consisting of two nitrogens and $N = 10$ protons (solid line) plotted as a function of the mismatch, that is the ratio $(\omega_I - \omega_S)/\omega_S$, where ω_S is the amplitude of the B_1 rf field (in frequency units) of the S-spin during the CP (exact match). As can be seen, the transferred intensity profile is asymmetric and has a higher efficiency at around 8% above the Hartmann–Hahn match than at
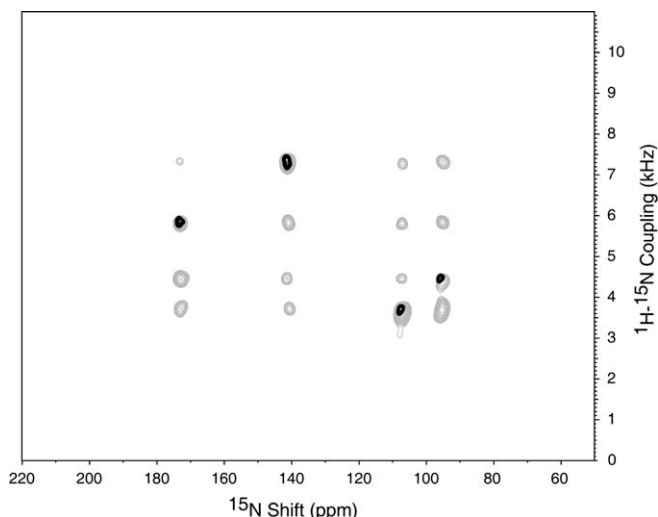

Fig. 2. Experimental solid-state NMR spectra acquired with a single ^{15}N-labeled n-acetyl Leucine crystal at arbitrary orientation using the pulse sequence of Fig. 1 (grey contour lines) overlaid with the corresponding SAMPI4 spectrum (black contour lines). The CP match rf field strength was 65 kHz (3.85 μs 90° pulse), 64 t_1 points were acquired in the indirect (dipolar) dimension; a 2-s Z-filter was applied, and the mixing time under the mismatched Hartmann–Hahn conditions was 7 ms. During the mixing, the proton rf amplitude was set to 70 kHz, i.e. at 8% above the CP match; 128 transients were acquired in the t_2 dimension with 6 sec recycle delay. A Bruker 3.2 mm MAS probe was used without the rotor spinning.
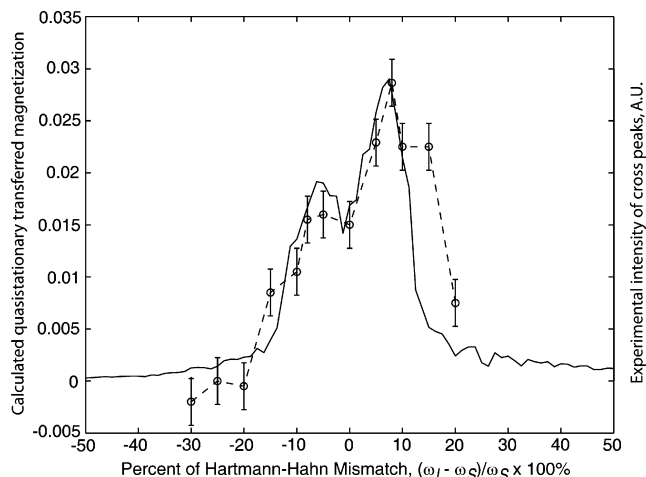
Fig. 3. Profiles of the maximum (quasistationary) transferred magnetization between two ^{15}N spins mediated by the proton network as a function of the Hartmann–Hahn mismatch. The simulation (solid line) was performed as described in the text. The left vertical axis was normalized relative to the initial magnetization of the first spin. Note the asymmetry in the profile for the transferred magnetization relative to the exact CP match. Circle-dashed line shows experimental intensities for one of the cross peaks at 142 ppm. The experimental intensities were uniformly scaled to best match the simulation. Error bars correspond to the noise level in the two-dimensional spectrum.

Fig. 4. Slices through the indirect dimension for the peak at 95 ppm obtained using the pulse sequence of Fig. 1 at the 8% mismatch above (solid line) and below (dashed line) relative to the CP match conditions. Other experimental conditions were as described in the legend for Fig. 2.

the same percentage below the match. The absolute values for the magnitude of the transferred magnetization most likely depend on the size and density of the spin system considered and, therefore, should be used for reference only. Nevertheless, this quantum-mechanical calculation correctly predicts the qualitative behavior of the transferred magnetization as a function of the Hartmann–Hahn mismatch when compared to the experimental profile. Fig. 3 also shows a plot of the experimental intensities for one representative cross-peak at 142 ppm (circle-dashed line). To estimate the intensity of the cross peaks, the background offset in the indirect dimension arising from the main peaks (which can be significant at larger mismatches) was subtracted from the cross-peak values. The experimental plot shows distinct asymmetry of the two maxima having higher values at positive mismatches, in agreement with the quantum-mechanical simulation. Moreover, the experimental intensity profile has the maximum values at around ±8% relative to the Hartmann–Hahn match, as predicted by the simulation. The relative efficiency of the transfer was also estimated experimentally by comparing the intensity of the cross peaks in the SAMPI4 exchanged spectra with the pure SAMPI4 spectrum run at exactly the same conditions (number of t_1 and t_2 points, scans, etc.) The intensity of the cross peaks for the various ^{15}N sites in the NAL sample was distributed between approximately 5% and 10% relative to the peaks in the SAMPI4 spectrum without the MMHH exchange, a somewhat larger value than predicted by the simulations with the finite number of protons considered (up to 3%). Fig. 4 shows representative slices through the indirect dimension corresponding to the peak at 95 ppm acquired at 8% above (solid line) and below (dashed line) the Hartmann–Hahn (or CP) match. The dipolar coupling corresponding to the main peak is indicated by arrows. As can be seen, setting the Hartmann–Hahn mismatch on the proton side above the exact value does increase the intensity of the cross peaks as predicted by the simulations. The spectral slices through the other three resonances exhibit the same trend (results not shown).

In conclusion, the magnetization transfer between dilute spins using the proton bath under mismatched Hartmann–Hahn condition opens up new strategies for NMR experiments that can be applied to static solid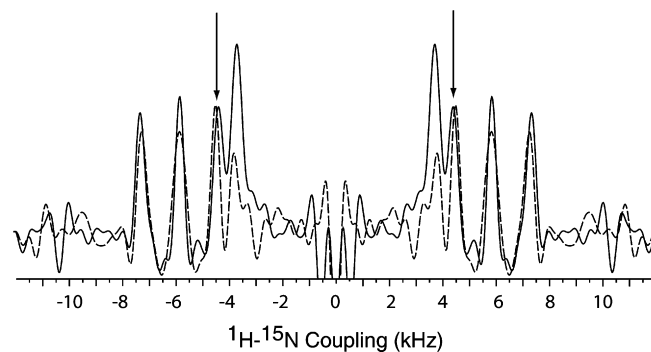s. Further experimental and theoretical research is needed to correlate the quasistationary amplitude of the transferred magnetization with the distance between the weak spins and the contact time. This may allow one to distinguish between close and distant spins in biological samples and establish a purely spectroscopic method of assignment.

Acknowledgments

References

[1] R.R. Ketcham, W. Hu, T.A. Cross, High-resolution conformation of gramidicin A in a lipid bilayer by solid-state NMR, Science 261 (1993) 1457–1460.

[2] J. Wang, S. Kim, F. Kovacs, T.A. Cross, Structure of the transmembrane region of the M2 protein H+ channel, Protein Sci. 10 (2001) 2241–2250.

[3] S.J. Opella, F.M. Marassi, J.J. Gesell, A.P. Valente, Y. Kim, M. Oblatt-Montal, M. Montal, Structures of the M2 channel-lining segments from nicotinic acetylcholine and NMDA receptors by NMR spectroscopy, Nat. Struct. Biol. 6 (1999) 374–379.

[4] F.M. Marassi, S.J. Opella, Simultaneous assignment and structure determination of a membrane protein from NMR orientational restraints, Protein Sci. 12 (2003) 403–411.

[5] A.C. Zeri, M.F. Mesleh, A.A. Nevzorov, S.J. Opella, Structure of the coat protein in fd filamentous bacteriophage particles determined by solid-state NMR spectroscopy, Proc. Natl. Acad. Sci. USA 100 (2003) 6458–6463.

[6] D.S. Thiriot, A.A. Nevzorov, L. Zagyanskiy, C.H. Wu, S.J. Opella, Structure of the coat protein in Pf1 bacteriophage determined by solid-state NMR spectroscopy, J. Mol. Biol. 341 (2004) 869–879.

[7] D.S. Thiriot, A.A. Nevzorov, S.J. Opella, Structural basis of the temperature transition of Pf1 bacteriophage, Protein Sci. 14 (2005).

[8] S.H. Park, A.A. Mrse, A.A. Nevzorov, M.F. Mesleh, M. Oblatt-Montal, M. Montal, S.J. Opella, Three-dimensional structure of the channel-forming trans-membrane domain of virus protein "u" (Vpu) from HIV-1, J. Mol. Biol. 333 (2003) 409–424.

[9] N.J. Traaseth, J.J. Buffy, J. Zamoon, G. Veglia, Structural dynamics and topology of phospholamban in oriented lipid bilayers using multidimensional solid-state NMR, Biochemistry 45 (2006) 13827–13834.

[10] A.A. De Angelis, S.C. Howell, A.A. Nevzorov, S.J. Opella, Structure determination of a membrane protein with two trans-membrane helices in aligned phospholipid bicelles by solid-state NMR spectroscopy, J. Am. Chem. Soc. 128 (2006) 12256–12267.

[11] F.M. Marassi, S.J. Opella, Using pisa pies to resolve ambiguities in angular constraints from PISEMA spectra of aligned proteins, J. Biomol. NMR 23 (2002) 239–242.

[12] D. Suter, R.R. Ernst, Spin diffusion in resolved solid-state NMR spectra, Phys. Rev. B 32 (1985) 5608–5627.

[13] F.M. Marassi, J.J. Gesell, A.P. Valente, Y. Kim, M. Oblatt-Montal, M. Montal, S.J. Opella, Dilute spin-exchange assignment of solid-state NMR spectra of oriented proteins: acetylcholine M2 in bilayers, J. Biomol. NMR 14 (1999) 141–148.

[14] J. Xu, J.S. Struppe, A. Ramamoorthy, Two-dimensional homonuclear chemical shift correlation established by the cross-relaxation driven spin diffusion in solids, J. Chem. Phys. 128 (2008) 052308.

[15] A.A. Nevzorov, Mismatched Hartmann–Hahn conditions cause proton-mediated intermolecular magnetization transfer between dilute low spin nuclei in NMR of static solids, J. Am. Chem. Soc. 130 (2008) 11282–11283.

[16] J.R. Lewandowski, G. De Paepe, G.P. Griffin, Proton assisted insensitive nuclei cross polarization, J. Am. Chem. Soc. 129 (2007) 728–729.

[17] J. Cavanagh, W.J. Fairbrother, A.G. Palmer, N.J. Skelton, Protein NMR Spectroscopy: Principles & Practice, Academic Press, San Diego, 1996.

[18] R.K. Hester, J.L. Ackerman, B.L. Neff, J.S. Waugh, Separated local field spectra in NMR – determination of structure in solids, Phys. Rev. Letts. 36 (1976) 1081–1083.

[19] C.H. Wu, A. Ramamoorthy, S.J. Opella, High-resolution heteronuclear dipolar solid-state NMR spectroscopy, J. Magn. Reson. A 109 (1994) 270–272.

[20] A.A. Nevzorov, S.J. Opella, Selective averaging for high-resolution solid-state NMR spectroscopy of aligned samples, J. Magn. Reson. 185 (2007) 59–70.

[21] B.M. Fung, A.K. Khitrin, K. Ermolaev, An improved broadband decoupling sequence for liquid crystals and solids, J. Magn. Reson. 142 (2000) 97–101.

[22] F.H. Allen, The Cambridge structural database: a quarter of a million crystal structures and rising, Acta Cryst. B 28 (2002) 380–388.